

## *d*-Wave–Induced Josephson Current Counterflow in YBa<sub>2</sub>Cu<sub>3</sub>O<sub>7</sub>/Nb Zigzag Junctions

H. J. H. Smilde, Ariando, D. H. A. Blank, G. J. Gerritsma, H. Hilgenkamp, and H. Rogalla

*Low Temperature Division, Department of Applied Physics and MESA<sup>+</sup> Research Institute,  
University of Twente, P.O. Box 217, 7500 AE Enschede, The Netherlands*

(Received 15 August 2001; published 23 January 2002)

Well-defined zigzag-shaped ramp-type Josephson junctions between YBa<sub>2</sub>Cu<sub>3</sub>O<sub>7</sub> and Nb have been studied. The magnetic field dependencies of the critical currents provide evidence for *d*-wave–induced alternations in the direction of the Josephson current between neighboring sides of the zigzag structure. The arrays present controllable model systems to study the influences of  $\pi$  facets in high-angle high- $T_c$  grain boundaries. From the characteristics, we estimate a possible imaginary *s*-wave admixture to the order parameter of the YBa<sub>2</sub>Cu<sub>3</sub>O<sub>7</sub> to be below 1%.

DOI: 10.1103/PhysRevLett.88.057004

PACS numbers: 74.20.Rp, 74.50.+r, 74.72.–h

Based on various studies, e.g., [1–4], in recent years the evidence for a predominant  $d_{x^2-y^2}$ -wave symmetry of the order parameter in the cuprate high- $T_c$  superconductors has accumulated [5]. With this symmetry, the superconducting wave function exhibits a  $\pi$ -phase difference for orthogonal directions in  $k$  space. From this, the intriguing possibility arises to configure superconducting circuits in which part of the Josephson junctions are biased with an additional  $\pi$ -phase shift ( $\pi$  junctions). Examples of circuits incorporating  $\pi$  junctions are corner junctions [3], tricrystal rings [2,4], and dc  $\pi$  SQUIDs [1,6,7]. In these structures, the  $\pi$  junctions are formed by connections between high- $T_c$  and low- $T_c$  superconductors, or by using grain boundaries prepared by employing specially designed tricrystalline or tetracrystalline substrates. Resulting from the geometrical limitations that are set by the use of such special substrates, and to the difficulties faced in preparing controllably high-quality junctions between high- $T_c$  and low- $T_c$  superconductors, more complex geometries have not been realized yet.

Multiple 0 and  $\pi$  junctions placed controllably at arbitrary positions would enable more detailed and systematic studies on the order parameter symmetry and its effects on Josephson devices, as well as the realization of theoretically proposed elements for superconducting (quantum)electronics [8–10]. It has been proposed, e.g., that the unusual behavior of high-angle grain boundary junctions in high- $T_c$  superconductors arises from regions along the interface that, due to their orientations, are characterized by an additional  $\pi$ -phase shift [11,12]. With this, the grain boundary junction as a whole can be envisaged as an array of 0 and  $\pi$  junctions. The unusual electronic properties of the grain boundary junctions include magnetic field dependencies of the critical current  $I_c(H_a)$  that deviate strongly from the standard Fraunhofer-like pattern and even show maxima at nonzero applied magnetic fields [13,14], the spontaneous generation of unquantized magnetic flux [15,16], and anomalous dependencies between the critical current and the gauge-invariant phase difference over the junctions [17,18]. The formation of the  $\pi$  regions in these grain

boundary junctions has been attributed to the combined effects of the predominant  $d_{x^2-y^2}$ -wave symmetry in the high- $T_c$  copper oxides and the faceted microstructure of the grain boundaries [11]. As this faceting is uncontrollable, such grain boundary junctions provide only limited possibilities for more detailed and systematic studies, e.g., on the effects of spatial correlations in the sign changes of the critical current densities on the electronic properties of the Josephson contacts [12].

In order to realize designed complex geometries incorporating many 0 and  $\pi$  junctions, sufficient flexibility and control is required in the positioning of the junctions. Furthermore, the junctions should be oriented such that their interface normal vectors have a component in the *ab* plane of the high- $T_c$  superconductor. A suitable way to achieve this is in an all-thin-film process using edge- [6] or ramp-type junctions between high- $T_c$  and low- $T_c$  superconductors.

Recently, we have established a method to fabricate high-quality ramp-type Josephson junctions between thin films of the high- $T_c$  and low- $T_c$  superconductors YBa<sub>2</sub>Cu<sub>3</sub>O<sub>7</sub> and Nb [19,20]. Here, we report the realization and characteristics of arrays of up to 80 contacts in the zigzag geometry shown in the inset of Fig. 1. Analogous to grain boundary junctions, the individual elements in the arrays are referred to as “facets.” Besides demonstrating the feasibility to realize complex thin film circuits consisting of a multitude of 0 and  $\pi$  junctions, such structures provide a means to derive an upper bound for a possible imaginary *s*-wave admixture to the order parameter symmetry of the YBa<sub>2</sub>Cu<sub>3</sub>O<sub>7</sub>.

In the employed configuration, all the facets are aligned along a  $\langle 100 \rangle$  direction of the YBa<sub>2</sub>Cu<sub>3</sub>O<sub>7</sub>, and are designed to have identical (absolute) values of the critical current densities  $J_c$ . The facets oriented along one direction are expected to exhibit an additional  $\pi$ -phase difference compared to those oriented in the other direction, due to a predominant  $d_{x^2-y^2}$  order parameter symmetry of YBa<sub>2</sub>Cu<sub>3</sub>O<sub>7</sub>. Consequently, the entire structure can be envisaged as a one-dimensional array of Josephson contacts with an alternating sign of  $J_c$ , i.e., exhibiting counterflow.

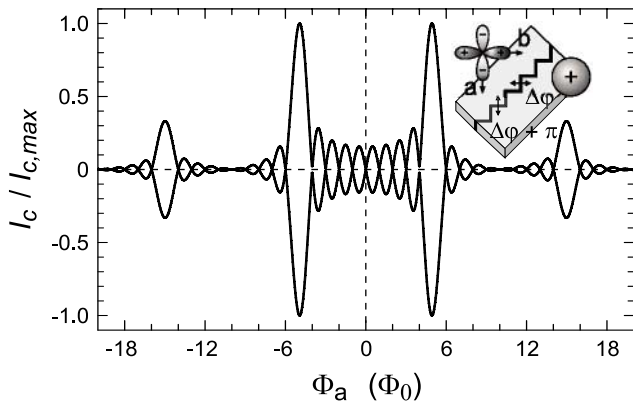


FIG. 1. Calculated magnetic flux dependence of the normalized critical current  $I_c/I_{c,\max}(\Phi_a)$  for an array of ten facets, composed of standard and  $\pi$ -Josephson contacts. The inset shows a schematic of the array, based on  $\text{YBa}_2\text{Cu}_3\text{O}_7/\text{Au}/\text{Nb}$  junctions.

In the following, before discussing the experiments, a brief theoretical background is provided on the expected magnetic flux dependence of the critical current for such arrays.

For a rectangular Josephson junction with dimensions comparable to, or smaller than, a few times the Josephson penetration depth  $\lambda_J$ , the influence of magnetic flux originating from applied bias currents up to the critical current  $I_c$  is negligible. In this,  $\lambda_J$  is given by  $\lambda_J = \sqrt{\hbar/2e\mu_0 J_c}$ , with  $t = \lambda_{L,1} + \lambda_{L,2} + d$  the magnetic barrier thickness;  $\lambda_{L,1}$  and  $\lambda_{L,2}$  are the effective London penetration depths of the two superconductors on either side of the junction, and  $d$  is the thickness of the barrier material. Under this condition, and presuming that along the junction the standard dc Josephson relation  $J = J_c \sin\Delta\varphi$  between the local supercurrent density  $J$  and the gauge-invariant phase

difference  $\Delta\varphi$  holds, the magnetic flux dependence of the critical current  $I_c$  of the junction is given by

$$I_c(\Phi) = J_c ha \left| \frac{\sin(\pi\Phi/\Phi_0)}{\pi\Phi/\Phi_0} \right|. \quad (1)$$

In this, the junction area equals  $A = ha$ , with  $h$  the effective junction height and  $a$  the junction width;  $\Phi$  denotes the magnetic flux coupled into the junction and  $\Phi_0$  is the flux quantum:  $2 \times 10^{-15} \text{ T m}^2$ . Equation (1) describes the well-known ‘‘Fraunhofer pattern,’’ which is the hallmark of small rectangular junctions with homogeneous current distributions.

The situation becomes somewhat more complicated for arrays of 0 and  $\pi$  junctions, for which the corner-junction configuration [21] represents the two-facet limit. The  $I_c(\Phi)$  dependence can be derived from the integral critical current distribution along the array,

$$I_c(\Phi) = \left| \sum_{n=1}^N \left( \int_{(n-1)a}^{na} J_c h e^{in\pi} e^{-i\beta x} dx \right) \right|, \quad (2)$$

where  $N$  is the number of facets with facet length  $a$ , and  $x$  is the coordinate of integration along the junction. The first exponent in this equation is related to the order parameter symmetry contribution to the phase difference along the junction, which varies between 0 and  $\pi$  every next facet. The term  $\beta x$  in the second exponent describes the phase difference at position  $x$  due to the applied magnetic flux, in the usual way. Assuming a constant coupling strength between the electrodes throughout the array, yielding a constant  $J_c$ , and a homogeneous distribution of magnetic flux, integration of Eq. (2) results in an analytic expression for the maximum supercurrent as a function of the magnetic flux as

$$I_c(\Phi) = \frac{J_c h N a}{2\pi\Phi/\Phi_0} \left\{ \left( \sum_{n=1}^N \sin \left[ n \left( \pi - \frac{2\pi}{\Phi_0} \frac{\Phi}{N} \right) \right] \left[ 1 - \cos \left( \frac{2\pi}{\Phi_0} \frac{\Phi}{N} \right) \right] - \cos \left[ n \left( \pi - \frac{2\pi}{\Phi_0} \frac{\Phi}{N} \right) \right] \sin \left( \frac{2\pi}{\Phi_0} \frac{\Phi}{N} \right) \right)^2 + \left( \sum_{n=1}^N \cos \left[ n \left( \pi - \frac{2\pi}{\Phi_0} \frac{\Phi}{N} \right) \right] \left[ 1 - \cos \left( \frac{2\pi}{\Phi_0} \frac{\Phi}{N} \right) \right] + \sin \left[ n \left( \pi - \frac{2\pi}{\Phi_0} \frac{\Phi}{N} \right) \right] \sin \left( \frac{2\pi}{\Phi_0} \frac{\Phi}{N} \right) \right)^2 \right\}^{1/2}. \quad (3)$$

The magnetic flux dependencies resulting from Eq. (3), of which an example is shown in Fig. 1, are identical to those derived by Mints and Kogan [12], who used an alternative approach.

Characteristic features of the  $I_c(\Phi)$  patterns for the arrays are the occurrence of sharp maxima in  $I_c$  for an applied magnetic flux  $\Phi_{\max} = N\Phi_0/2$ , and the vanishing  $I_c$  at  $\Phi = 0$  for an even number of facets. Further, the number of minima in  $I_c$  in the flux range  $-\Phi_{\max} < \Phi < \Phi_{\max}$  is predicted to equal  $N - 1$ . It is to be noted that in this analysis possible self-generated magnetic flux is not taken into account, which becomes important if the facet length is significant in comparison with the local Josephson penetration depth [16,22].

For the preparation of  $\text{YBa}_2\text{Cu}_3\text{O}_7/\text{Au}/\text{Nb}$  junctions, bilayers of 150 nm [001]-oriented  $\text{YBa}_2\text{Cu}_3\text{O}_7$  and 100 nm  $\text{SrTiO}_3$  were grown by pulsed-laser deposition on edge-aligned [001]-oriented  $\text{SrTiO}_3$  single crystal substrates, and zigzag structures were ion milled under an angle with the substrate plane yielding a ramp with a slope of  $15^\circ$ – $20^\circ$ . The in-plane velocity components of the incident Ar ions were oriented along the  $\text{YBa}_2\text{Cu}_3\text{O}_7$   $\langle 110 \rangle$ -direction, in order to create identical circumstances for all facets. Then, a 6 nm  $\text{YBa}_2\text{Cu}_3\text{O}_7$  interlayer is prepared, providing for a high-quality interface to the subsequently *in situ* deposited 14 nm Au-barrier layer. After preparation of the Au-barrier layer, a 140 nm Nb

layer is deposited by dc sputtering. For further details concerning the properties of junctions prepared in this way, we refer to [20].

The measurements have been performed by a four-probe method in a well-shielded liquid-helium cryostat ( $T = 4.2$  K). In all cases, the magnetic field  $H_a$  was applied along the [001]-direction of the  $\text{YBa}_2\text{Cu}_3\text{O}_7$  unit cell. Critical currents were measured with a voltage bias below  $5 \mu\text{V}$ . Variations of the bias voltage in this range did not affect the basic features in the  $I_c(H_a)$  characteristics.

Figure 2 shows a typical  $I(V)$  characteristic and  $I_c(H_a)$  dependence of a single  $\text{YBa}_2\text{Cu}_3\text{O}_7/\text{Au}/\text{Nb}$  Josephson junction. The  $I(V)$  characteristic is hysteretic, which is indicated in the  $I_c(H_a)$  dependence with the black area. The magnetic flux dependence resembles closely the Fraunhofer pattern described by Eq. (1), with a maximum in the critical current of  $I_c = 6.5 \mu\text{A}$ , corresponding to  $J_c = 90 \text{ A/cm}^2$ , at zero applied magnetic flux. From this, the Josephson penetration depth  $\lambda_J$  for these junctions is estimated to be approximately  $40 \mu\text{m}$ . The normal state resistance  $R_n$  of this junction equals  $20 \Omega$ .

Figure 3(a) presents the  $I_c(H_a)$  dependence for an array of eight facets of each  $25 \mu\text{m}$  width, placed in the zigzag geometry of the inset of Fig. 1. Clearly, the maxima in the critical current are now observed at a nonzero applied magnetic flux,  $H_a = 1.1 \mu\text{T}$ . At this field value  $I_c$  equals  $50 \mu\text{A}$ . The  $R_n$  value is  $1.5 \Omega$ . In Fig. 3(b), the magnetic field dependence of the critical current is shown for an array of 80 facets of  $5 \mu\text{m}$  width. Even these very complex arrays show highly symmetric patterns with maxima occurring at nonzero applied magnetic field, namely,  $I_c = 41 \mu\text{A}$  at  $H_a = 5.1 \mu\text{T}$ . For this array, the  $R_n$  also equals  $1.5 \Omega$ . The ratios between the  $I_c$  values at zero magnetic field and the maximal critical currents are 17% and 27% for the arrays shown in Figs. 3(a) and 3(b), respectively. For an array of ten facets of  $40 \mu\text{m}$  width, not shown here, a ratio as small as 6% was found.

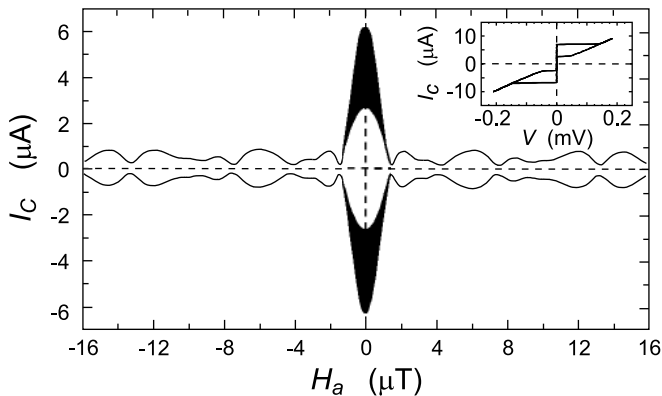


FIG. 2. Critical current  $I_c$  as a function of applied magnetic flux  $H_a$  for a  $50 \mu\text{m}$  wide  $\text{YBa}_2\text{Cu}_3\text{O}_7/\text{Au}/\text{Nb}$  ramp-type junction, for positive and negative bias voltage of  $2.5 \mu\text{V}$ . The dark area indicates the hysteresis in the current-voltage ( $I$ - $V$ ) characteristic. The inset presents an  $I$ - $V$  characteristic for the same junction.

Clearly, the field dependencies of the critical currents for the arrays display the characteristic features indicated by Fig. 1, namely, the absence of a global maximum at  $H_a = 0$  and the sharp increases in the critical current at a given applied magnetic field. This behavior can be explained only by the arrays being comprised of facets alternately biased with or without an additional  $\pi$ -phase change. As all facets are aligned along the  $\langle 100 \rangle$  axes of the  $\text{YBa}_2\text{Cu}_3\text{O}_7$  and were prepared in an identical way, intrinsic processes at the interfaces cannot be the cause of these  $\pi$ -phase shifts, and the results thus provide further compelling evidence for a predominant  $d_{x^2-y^2}$  symmetry of the order parameter in the high- $T_c$  cuprate. The normal state resistances indicate slight variations in the interface transparencies for the different junctions, which are positioned several mm apart. Such variations are not uncommon for junctions involving high- $T_c$  superconductors.

Because of the orthorhombicity of  $\text{YBa}_2\text{Cu}_3\text{O}_7$ , subdominant order parameter components may be expected to arise, e.g., as real or imaginary  $s$ -wave admixtures to the  $d_{x^2-y^2}$  symmetry. Various experiments are currently undertaken to study such possible admixtures, often relying on tunneling along the  $\langle 110 \rangle$  direction of the  $\text{YBa}_2\text{Cu}_3\text{O}_7$ , which is the nodal direction of the  $d_{x^2-y^2}$  symmetry component. In such a configuration, it is difficult to distinguish

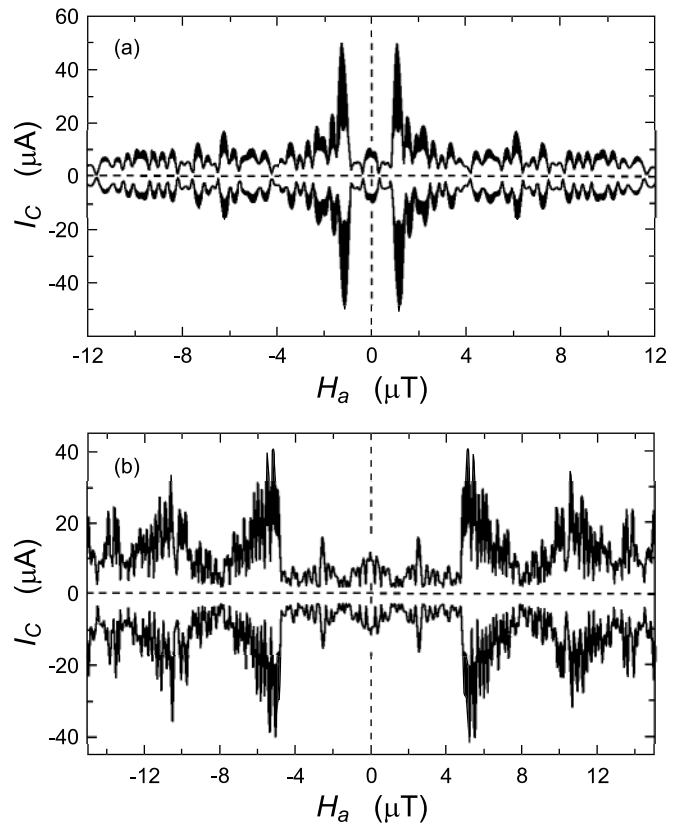


FIG. 3. Critical current  $I_c$  as a function of applied magnetic flux  $H_a$  for (a) an array of eight alternating 0 and  $\pi$  facets of  $25 \mu\text{m}$  width ( $V_{\text{bias}} = 1 \mu\text{V}$ ), and (b) an array of 80 alternating 0 and  $\pi$  facets of  $5 \mu\text{m}$  width ( $V_{\text{bias}} = 5 \mu\text{V}$ ).

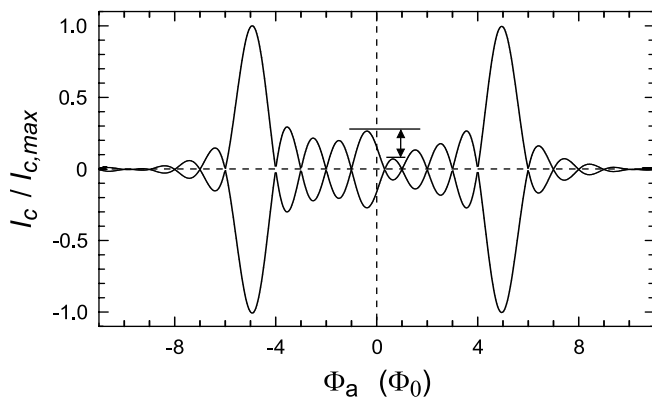


FIG. 4. Calculated  $I_c/I_{c,\max}(\Phi_a)$  dependence for an array of ten facets, presuming the order parameter symmetry to be  $d_{x^2-y^2} + 0.1is$ . The imaginary  $s$ -wave induces asymmetries in the  $I_c/I_{c,\max}(\Phi_a)$  dependence, especially around  $\Phi_a = 0$ , as is indicated with the arrow.

whether possible subdominant components are intrinsic to the superconductivity in the  $\text{YBa}_2\text{Cu}_3\text{O}_7$ , or whether they are induced only locally by the particularities connected with the  $\langle 110 \rangle$  interfaces, e.g., the presence of Andreev bound states [23,24]. Therefore, order parameter symmetry test experiments that avoid such  $\langle 110 \rangle$  surfaces, as is the case for the arrays described here, are of particular interest. If the order parameter were to comprise an imaginary  $s$ -wave admixture, the  $I_c(H_a)$  dependencies for the arrays would be expected to display distinct asymmetries, especially for low fields (see Fig. 4). From the high degree of symmetry of the measured characteristics [Figs. 3(a) and 3(b)], we conclude that, if there is an imaginary  $s$ -wave contribution, it will be smaller than 1%. We note that due to the twinning in the films no conclusion can be drawn about possible real  $s$ -wave admixtures. Furthermore, the presented configuration is insensitive to possible admixtures of subdominant  $d_{xy}$  components, as all facets face a nodal direction of this symmetry component.

The  $I_c(H_a)$  characteristics of the arrays resemble in their basic features the ones observed for asymmetric  $45^\circ$  [001]-tilt grain boundary junctions [11,14]. This strongly supports the hypothesis that the anomalous characteristics for these grain boundary junctions are due to the occurrence of regions with additional  $\pi$ -phase shifts along the interface.

Additionally, the influence of flux focusing, creating a nonhomogeneous flux coupling to the junction [25,26] is clearly visible in the characteristics of the arrays. The local flux coupled to the junction is expected to be larger in the center of the array than at the edges. As a result, the shape of the major peak displays a sharp enhancement in the critical current when reaching  $H_{\max}$ , followed by a more shallow decrease in  $I_c$  for larger applied fields. The

effects become more pronounced for an increasing number of facets in the arrays.

In conclusion, the realization and characteristics of zigzag-shaped  $\text{YBa}_2\text{Cu}_3\text{O}_7/\text{Au}/\text{Nb}$  junctions are described. The  $I_c(H_a)$  dependencies of these structures provide evidence for a Josephson current counterflow, in agreement with a predominant  $d_{x^2-y^2}$ -wave order parameter symmetry of the  $\text{YBa}_2\text{Cu}_3\text{O}_7$ . The highly symmetric  $I_c(H_a)$  characteristics indicate that a possible subdominant imaginary  $s$ -wave admixture to the order parameter symmetry is below 1%.

The authors thank A. A. Golubov, D. J. van Harlingen, J. Mannhart, R. G. Mints, C. W. Schneider, and C. C. Tsuei for valuable discussions. This work was supported by the Dutch Foundation for Research on Matter (FOM) and the Royal Dutch Academy of Arts and Sciences (KNAW).

- [1] D. A. Wollman *et al.*, Phys. Rev. Lett. **71**, 2134 (1993).
- [2] C. C. Tsuei *et al.*, Phys. Rev. Lett. **73**, 593 (1994).
- [3] D. J. van Harlingen, Rev. Mod. Phys. **67**, 515 (1995).
- [4] J. R. Kirtley *et al.*, Nature (London) **373**, 225 (1995).
- [5] C. C. Tsuei and J. R. Kirtley, Rev. Mod. Phys. **72**, 969 (2000).
- [6] A. Mathai *et al.*, Phys. Rev. Lett. **74**, 4523 (1995).
- [7] R. R. Schulz *et al.*, Appl. Phys. Lett. **76**, 912 (2000).
- [8] E. Terzioglu and M. R. Beasley, IEEE Trans. Appl. Supercond. **8**, 48 (1998).
- [9] L. B. Ioffe *et al.*, Nature (London) **398**, 679 (1999).
- [10] G. Blatter, V. B. Geshkeinbein, and L. B. Ioffe, Phys. Rev. B **63**, 174511 (2001).
- [11] H. Hilgenkamp, J. Mannhart, and B. Mayer, Phys. Rev. B **53**, 14 586 (1996).
- [12] R. G. Mints and V. G. Kogan, Phys. Rev. B **55**, R8682 (1997).
- [13] C. A. Copetti *et al.*, Physica (Amsterdam) **253C**, 63 (1995).
- [14] J. Mannhart, B. Mayer, and H. Hilgenkamp, Z. Phys. B **101**, 175 (1996).
- [15] J. R. Kirtley *et al.*, Phys. Rev. B **51**, 12 057 (1995).
- [16] J. Mannhart *et al.*, Phys. Rev. Lett. **77**, 2782 (1996).
- [17] E. Il'ichev *et al.*, Phys. Rev. Lett. **81**, 894 (1998).
- [18] E. Il'ichev *et al.*, Phys. Rev. Lett. **86**, 5369 (2001).
- [19] H. J. H. Smilde *et al.*, Physica (Amsterdam) **350C**, 269 (2001).
- [20] H. J. H. Smilde *et al.*, IEEE Trans. Appl. Supercond. **11**, 501 (2001).
- [21] D. A. Wollman *et al.*, Phys. Rev. Lett. **74**, 797 (1995).
- [22] R. G. Mints and I. Papiashvili, Phys. Rev. B **62**, 15 214 (2000).
- [23] C. R. Hu, Phys. Rev. Lett. **72**, 1526 (1994).
- [24] S. Kashiwaya and Y. Tanaka, Rep. Prog. Phys. **63**, 1641 (2000).
- [25] P. A. Rosenthal *et al.*, Appl. Phys. Lett. **59**, 3482 (1991); **60**, 1591 (1992).
- [26] R. G. Humphreys and J. A. Edwards, Physica (Amsterdam) **210C**, 42 (1993).